Delft University of Technology

Attitude Estimation of a Quadcopter with one fully damaged rotor using on-board MARG Sensors

Solanki, P.; de Visser, C.C.

DOI
10.2514/6.2022-0857

Publication date
2022

Document Version
Final published version

Published in
AIAA SCITECH 2022 Forum

Citation (APA)
Solanki, P., & de Visser, C. C. (2022). Attitude Estimation of a Quadcopter with one fully damaged rotor using on-board MARG Sensors. In *AIAA SCITECH 2022 Forum* Article AIAA 2022-0857 (AIAA Science and Technology Forum and Exposition, AIAA SciTech Forum 2022). https://doi.org/10.2514/6.2022-0857

Important note
To cite this publication, please use the final published version (if applicable).
Please check the document version above.

Copyright
Other than for strictly personal use, it is not permitted to download, forward or distribute the text or part of it, without the consent of the author(s) and/or copyright holder(s), unless the work is under an open content license such as Creative Commons.

Takedown policy
Please contact us and provide details if you believe this document breaches copyrights.
We will remove access to the work immediately and investigate your claim.

This work is downloaded from Delft University of Technology.
For technical reasons the number of authors shown on this cover page is limited to a maximum of 10.

AIAA SciTech Forum
January 3-7, 2022, San Diego, CA & Virtual
AIAA SCITECH 2022 Forum

10.2514/6.2022-0857

Attitude Estimation of a Quadcopter with one fully damaged rotor using on-board MARG Sensors

Prashant Solanki[1], C.C. de Visser[2]

***Abstract*— Quadcopters are becoming increasingly popular across diverse sectors. Since rotor damages occur frequently, it is essential to improve the attitude estimation and thus ultimately the ability to control a damaged quadcopter. This research is based on a state-of-the-art method that makes it possible to control the quadcopter despite the total failure of a single rotor, where the attitude and position of the quadcopter are provided by an external system. In the present research, a novel attitude estimator called Adaptive Fuzzy Complementary Kalman Filter (AFCKF) has been developed and validated that works independently of any external systems. It is able to estimate the attitude of a quadcopter with one fully damaged rotor while only relying on the on-board MARG (Magnetometer, Accelerometer, Rate Gyroscope) sensors. The AFCKF provides significantly better attitude estimates for flights with a damaged rotor than mainstream filters, estimating the roll and pitch of the quadcopter with an RMS error of less than 1.7 degrees and a variance of less than 2 degrees. The proposed filter also provides accurate yaw estimates despite the fast spinning motion of the damaged quadcopter, and thus outperforms existing methods at the cost of only a small increase in computation.**

I. Introduction

By virtue of mechanical simplicity, quadcopters have become very popular in multiple industries. A wide range of research has been conducted to develop a fault-tolerant controller for a quadcopter subjected to rotor failure ([1], [2]). In the scenario of a complete single rotor failure, the quadcopter has to abandon yaw control and spin at a high angular rate, which introduces high centrifugal accelerations and is thus detrimental to conventional on-board attitude estimation methods.

This research is based on a fault-tolerant controller developed by [2] for a quadcopter subjected to a complete single rotor failure. The attitude of that quadcopter was attained using a motion-capture system. Unfortunately, no such motion capture system exists for the outside environment. There exist a wide spectrum of attitude estimation techniques based on different approaches to cater for this problem. One category are stochastic estimation techniques which are based on Kalman Filters or Extended Kalman Filters (EKF), such as [3], [4], [5], [6]. The issue with Kalman-based estimators is that they tend to be computationally heavy and are affected by linearization errors. Another approach is based on Wahba's problem ([7]), which inspired filters such as [8], [9], and [10]. These filters tend to be highly susceptible to noise, which means that applying them on low-cost sensors can lead to high estimation errors. Lastly, complementary filter based methods such as [11], [12] and, [13] tend to be computationally lighter and are developed for low-cost MARG sensors, but they too are adversely affected by magnetic distortions and external accelerations.

Consequently, none of these attitude estimation techniques are able to perform sufficiently well under highly dynamic motion such as is the case when one rotor is fully damaged and the quadcopter rotates about the yaw axis. Thus, the present research develops an attitude estimation method that can estimate the states of the quadcopter with a damaged rotor with sufficient accuracy while using only the on-board MARG (magnetometer, accelerometer, rate gyroscope) sensors and is consequently suitable for an outside environment. Section II of this paper explains the chosen quaternion representation scheme; section III the filter design, and section IV the results and discussion.

II. Quaternion representation scheme

The AFCKF is based on the quaternion representation of the attitude. $q_{A/B}$ provides the orientation of the frame B with respect to frame A. The quaternion is defined as shown in equation 1, with r_A being a unit vector as shown by equation 2.

$$q_{A/B} = \begin{bmatrix} q_1 \\ q_2 \\ q_3 \\ q_4 \end{bmatrix}^T = \begin{bmatrix} cos(\theta/2) \\ -r_x sin(\theta/2) \\ -r_y sin(\theta/2) \\ -r_z sin(\theta/2) \end{bmatrix}^T \tag{1}$$

$$r_A^2 = r_x^2 + r_y^2 + r_z^2 \tag{2}$$

Quaternions are constrained to be normalised as shown in equation 3, where q^T is the quaternion transpose.

$$qq^T = q_1^2 + q_2^2 + q_3^2 + q_4^2 = 1 \tag{3}$$

The quaternion conjugate, denoted with $'*'$ on the superscript, describes the orientation of frame A with respect to frame B and is given by equation 4.

$$q_{B/A} = q_{A/B}^* = \begin{bmatrix} q_1 & -q_2 & -q_3 & -q_4 \end{bmatrix} \tag{4}$$

The quaternion product is used to find the compound orientation. If two quaternions $q_{B/C}$ and $q_{A/B}$ are known, then $q_{A/C}$ can be found using equation 5 ([14]). The quaternion product can be obtained using the Hamilton theorem, given by equation 6. The quaternion product is not commutative, i.e., $q_{B/C} \otimes q_{A/B} \neq q_{A/B} \otimes q_{B/C}$.

$$q_{A/C} = q_{B/C} \otimes q_{A/B} \tag{5}$$

Downloaded by TU DELFT on January 5, 2022 | http://arc.aiaa.org | DOI: 10.2514/6.2022-0857

Copyright © 2022 by Prashant Solanki, Coen de Visser. Published by the American Institute of Aeronautics and Astronautics, Inc., with permission.

Downloaded by TU DELFT on January 5, 2022 | http://arc.aiaa.org | DOI: 10.2514/6.2022-0857

$$p \otimes r = \begin{bmatrix} p_1 \\ p_1 \\ p_3 \\ p_4 \end{bmatrix}^T \otimes \begin{bmatrix} r_1 \\ r_2 \\ r_3 \\ r_4 \end{bmatrix}^T = \begin{bmatrix} p_1 r_1 - p_2 r_2 - p_3 r_3 - p_4 r_4 \\ p_1 r_2 + p_2 r_1 + p_3 r_4 - p_4 r_3 \\ p_1 r_3 - p_2 r_4 + p_3 r_1 + p_4 r_2 \\ p_1 r_4 + p_2 r_3 - p_3 r_2 + p_4 r_1 \end{bmatrix}^T \tag{6}$$

If $q_{A/B}$ is known, then a three-dimensional vector in frame A ($\vec{v}^A$) can be converted into frame B using equation 7. An additional zero is added as the fourth element of the vector in frame A ($\vec{v}^A$) and in frame B ($\vec{v}^B$).

$$\begin{bmatrix} 0 & \vec{v}^B \end{bmatrix} = q_{A/B} \otimes \begin{bmatrix} 0 & \vec{v}^A \end{bmatrix} \otimes q^*_{A/B} \tag{7}$$

Equation 7 can be represented in the form of a rotation matrix ($C_{B/A}$) as shown in equation 8 ([14]), where $C_{B/A}$ is the rotation matrix that transforms the vectors in frame A into the vectors in frame B.

$$C_{B/A} = \begin{bmatrix} -1+2(q_1^2+q_2^2) & 2(q_2q_3+q_4q_1) & 2(q_2q_4-q_3q_1) \\ 2(q_2q_3-q_4q_1) & -1+2(q_1^2+q_3^2) & 2(q_3q_4+q_2q_1) \\ 2(q_2q_4+q_3q_1) & 2(q_3q_4-q_2q_1) & -1+2(q_1^2+q_4^2) \end{bmatrix} \tag{8}$$

The relationship between the quaternion and Euler angles, i.e., roll angle (ϕ), pitch angle (θ) and yaw angle (ψ), is given by equation 9.

$$\phi = tan^{-1}\left\{\frac{2(q_3q_2-q_1q_4)}{1-2q_1^2 2q_2^2}\right\} \tag{9}$$

$$\theta = sin^{-1}\{2(q_2q_4+q_1q_3)\}$$

$$\psi = tan^{-1}\left\{\frac{2(q_2q_3-q_1q_2)}{2q_1^2 2q_4^2-1}\right\}$$

III. Filter Derivation

In this section, the filter is derived and presented along with the equations of the attitude estimator. The schematics of the AFCKF are shown in figure 1. For a better understanding, the AFCKF is divided into five parts.

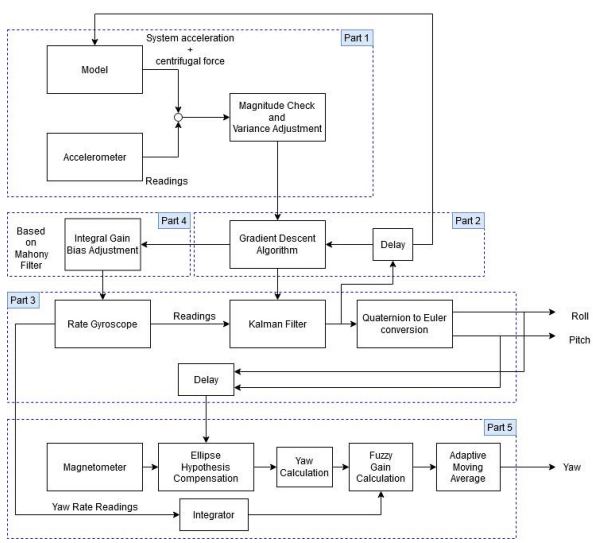

Fig. 1. Schematics of the AFCKF

A. Correcting the accelerometer readings

The ideal measurement model of an accelerometer in space is given by equation 10, where $\vec{a}_B$ is the acceleration of the body, $\vec{r}_B$ is the position vector of the accelerometer from the center of rotation, $\vec{\omega}_B$ is the rotational velocity of the body reference frame, $2\vec{\omega}_B \times \dot{\vec{r}}_B$ is the Coriolis acceleration (which is zero in the case of a fixed sensor), $\vec{g}_B$ is the gravity vector in the body frame of reference, $\vec{\omega}_B \times (\vec{\omega}_B \times \vec{r}_B)$ is the centrifugal acceleration and $\dot{\vec{\omega}}_B \times \vec{r}_B$ is zero under the assumption that $\dot{\vec{\omega}}_B$ is zero for a quadcopter. Furthermore, the accelerometer readings are corrupted with noise denoted by e_a and bias denoted by $\delta_{a,t}$. The noise is assumed to be zero mean white Gaussian noise with a standard deviation Σ_a, as given by equation 12. Equation 10 reduces to 11 due to the aforementioned reasons.

$$\vec{a}_{B_{measured}} = \vec{a}_B + \dot{\vec{\omega}}_B \times \vec{r}_B + 2\vec{\omega}_B \times \dot{\vec{r}}_B + \vec{\omega}_B \times (\vec{\omega}_B \times \vec{r}_B) + \vec{g}_B \tag{10}$$

$$\vec{a}_{B_{measured}} = \vec{a}_B + \vec{\omega}_B \times (\vec{\omega}_B \times \vec{r}_B) + \vec{g}_B + e_a + \delta_{a,t} \tag{11}$$

$$\Sigma_a = \begin{bmatrix} \sigma_{acc_x} & 0 & 0 \\ 0 & \sigma_{acc_y} & 0 \\ 0 & 0 & \sigma_{acc_z} \end{bmatrix} \tag{12}$$

In order to obtain correct attitude estimates, the accelerometer readings must be dominated by the gravity vector. However, the quadcopter's linear acceleration and the centrifugal acceleration are also measured by the accelerometer and thus need to be accounted for. These external noises are modeled using a predetermined model. The estimator is designed in such a way that only a crude model of the centrifugal force about the z-axis is required, which is given by equation 13, where ω_z^2 is the yaw rate of the quadcopter, and ϖ_1 and ϖ_2 are constants. The value of the constants is determined in the sensor calibration routine. The centrifugal force is only modeled about the body frame z-axis because the controller developed by [2] rotates about the body frame yaw axis after the rotor damage occurs.

$$\vec{a}_{C_B} = \begin{bmatrix} \vec{F}_{C_{B_x}} & \vec{F}_{C_{B_y}} & \vec{F}_{C_{B_z}} \end{bmatrix} = \omega_z^2 \cdot \begin{bmatrix} \varpi_1 & \varpi_2 & 0 \end{bmatrix} \tag{13}$$

Furthermore, it is assumed that the linear acceleration of the quadcopter is short-lived and small compared to the acceleration due to gravity. Thus, after the centrifugal acceleration is compensated for, the measured acceleration is given by equation 14. The obtained accelerometer reading is normalised against the gravity vector as given by equation 15, where g is the acceleration due to gravity.

$$\vec{a}_{B_{corrected}} = \vec{a}_{B_{measured}} - \vec{a}_{C_B} \tag{14}$$

$$\vec{a}_{cor} = \frac{\vec{a}_{B_{corrected}}}{|g|} \tag{15}$$

Downloaded by TU DELFT on January 5, 2022 | http://arc.aiaa.org | DOI: 10.2514/6.2022-0857

B. Obtaining the attitude from the accelerometer reading

If magnitude and direction of a field in the earth frame are known, the attitude of the body frame relative to the earth can be calculated using an observation of the corresponding field in the sensor/body frame. However, the calculated orientation is not unique. There exist infinite solutions represented by rotating the true attitude about an axis parallel to the direction of the field in the earth frame. Thus, since only accelerometer readings are used to obtain an attitude estimate, the corresponding yaw estimates cannot be trusted (because the gravity vector runs parallel to the earth frame's yaw axis). This attitude estimation problem can be converted into an optimisation problem where a rotation operation, given by equation 7, aligns the known field in the earth frame, $\hat{v}$, to the corresponding measurement of the field in the sensor frame, $\hat{s}$, thus providing the attitude of the sensor with respect to the inertial frame. An optimisation algorithm scheme is formulated to acquire an attitude estimate. The minimisation function is given by equation 16.

$$min[f(q,\hat{v},\hat{s})] \tag{16}$$

$$f(q,\hat{v},\hat{s}) = q^*_{t-1} \otimes \hat{v} \otimes q_{t-1} - \hat{s}$$

$$\hat{v} = \begin{bmatrix} 0 & v_x & v_y & v_z \end{bmatrix}$$

$$\hat{s} = \begin{bmatrix} 0 & s_x & s_y & s_z \end{bmatrix}$$

The gradient descent algorithm is used for optimising and obtaining an attitude estimate. This method is chosen for the purpose of optimisation because of its low computational cost and simplicity. The algorithm is given by equations 17 and 18, used for obtaining the attitude estimate q_n, given the initial estimate q_0, where n is the number of iterations, $\hat{v}$ is the field vector in the earth frame with an added null dimension, $\hat{s}$ consists of the measurement of the field in the sensor frame with an added null dimension, and μ is the step size. The optimal value of the step size ensures the convergence of the q_k. The quaternions are re-normalised after every time step to ensure property 3.

$$q_k = q_{k-1} - \mu \frac{\nabla f(q_{k-1},\hat{v},\hat{s})}{||\nabla f(q_{k-1},\hat{v},\hat{s})||}, k = 1,2...n \tag{17}$$

$$\nabla f(q_{k-1},\hat{v},\hat{s}) = J^T(q_{k-1},\hat{v}) f(q_{k-1},\hat{v},\hat{s}) \tag{18}$$

For the AFCKF, the known field is the acceleration due to gravity, which is having components along only one principle axis of the earth frame. Equations 19 and 20 give the normalised gravity field with an added null dimension and the normalised corrected accelerometer readings with an added null dimension respectively. Equations 21 and 22 give the minimisation function and its Jacobian respectively.

$$\hat{g} = \begin{bmatrix} 0 & 0 & 0 & 1 \end{bmatrix} \tag{19}$$

$$\hat{a}_{cor} = \begin{bmatrix} 0 & a_{cor_x} & a_{cor_y} & a_{cor_z} \end{bmatrix} \tag{20}$$

$$f_g(q,\hat{g},\hat{a}) = \begin{bmatrix} 2(q_2q_4 - q_1q_3) - a_{cor_x} \\ 2(q_2q_1 + q_4q_3) - a_{cor_y} \\ 2(\frac{1}{2} - q_2^2 - q_3^2) - a_{cor_z} \end{bmatrix} \tag{21}$$

$$J_g^T(q,\hat{g}) = \begin{bmatrix} -2q_3 & 2q_4 & -2q_1 & 2q_2 \\ 2q_2 & 2q_1 & 2q_4 & 2q_3 \\ 0 & -4q_2 & -4q_3 & 0 \end{bmatrix} \tag{22}$$

Equation 23 provides the attitude estimate at the current time step given the optimum attitude estimate of previous time steps and the current accelerometer reading. $q_{\nabla,t}$ is the attitude estimate of the current time step obtained using the gradient descent algorithm.

$$q_{\nabla,t} = q_{t-1} - u_t \frac{\nabla f_g}{||\nabla f_g||} \tag{23}$$

$$\nabla f_g = J_g^T(q_{t-1},\hat{g}) f_g(q_{t-1},\hat{g},\hat{a}_{cor_t})$$

The convergence of the optimisation process depends on the value of the step size (μ_t). A typical optimisation approach needs multiple iterations to obtain a new attitude estimate given a new accelerometer observation. To increase the efficiency of the optimisation process, the step size (μ_t) needs to be adjusted at every time step. If the convergence rate is equal to or higher than the physical rate of change of the attitude, then only one iteration per sample time is enough to obtain an attitude estimate with sufficient accuracy. Since the convergence rate is governed by μ_t, the appropriate value of μ_t can ensure that the convergence of the attitude is limited by the physical rate of change of the attitude, avoiding overshooting. The value of μ_t is given by equation 24, where β is a scaling constant that accounts for accelerometer noise, $\dot{q}_{\omega,t}$ is the current physical rate of change of the attitude (measured by the gyroscope) and Δt is the time step.

$$\mu_t = \beta |\dot{q}_{\omega,t}| \Delta t, \beta > 1 \tag{24}$$

This process ensures that the step size is adapted according to the physical rate of change of the attitude.

C. Optimal roll and pitch estimates using the Kalman filter

The rate gyroscope measures the quadcopter's angular rate (angular velocity) with respect to the inertial frame represented in the body frame of reference. The angular rate is used to obtain the rate quaternion ($\dot{q}$) using equation 25 ([15]), where ω_t is the current time step gyro reading and q_{t-1} is the previous time step optimum attitude estimate.

$$\dot{q}_{\omega,t} = \frac{1}{2} q_{t-1} \otimes \begin{bmatrix} 0 & \omega_{x_t} & \omega_{y_t} & \omega_{z_t} \end{bmatrix} \tag{25}$$

Given the previous time step optimum attitude estimate and Δt, a numerical integration can be used to obtain the current time step attitude. This is shown in equation 26, where $q_{\omega,t}$ is the attitude estimate obtained from the gyroscope.

$$q_{\omega,t} = q_{t-1} + \dot{q}_{\omega,t} \Delta t \tag{26}$$

An extended Kalman filter (see the algorithm below) is used to obtain the optimum roll and pitch estimates of the quadcopter. The Kalman filter consists of a process model and a sensor model.

Downloaded by TU DELFT on January 5, 2022 | http://arc.aiaa.org | DOI: 10.2514/6.2022-0857

1) Process model: The process model of the Kalman filter consists of the gyroscope readings and is given by equations 25 and 26. The gyroscope is used to obtain the angular rate of the quadcopter. However, gyroscope readings are corrupted by noise and bias. The stationary bias (δ_ω) is removed from the gyroscope readings through calibration. The gyroscope noise, e_ω, is assumed to be Gaussian distributed white noise with zero mean and a known standard deviation given by equation 27. It is also assumed that there is no correlation between the noise of the three gyroscope axis readings. Furthermore, the gyroscope is plagued with a bias drift. Thus, after the stationary bias correction, the gyroscope measurements consist of real angular velocity (ω) that is unknown, gyro noise (e_ω), and the gyro bias drift (b_{ω_t}) as shown in equation 28.

$$\Sigma_\omega = \begin{bmatrix}\sigma_{\omega_x} & \sigma_{\omega_y} & \sigma_{\omega_z}\end{bmatrix} I_{3\times3} \tag{27}$$

$$\omega_{gyro_t} = \omega_t + e_\omega + b_{\omega_t} \tag{28}$$

The gyroscope readings are corrected for the bias drift using an orientation filter based on the feedback of the error in the rate of attitude change, as is shown in the later section of this paper. Thus, after the bias drift correction and using equation 25, 26, and 28, the process mode is given by equation 29.

$$q_{\omega,t} = q_{t-1} + \frac{1}{2} q_{t-1} \otimes \left(\begin{bmatrix}0 & \omega_t\end{bmatrix} + \begin{bmatrix}0 & e_\omega\end{bmatrix}\right)\Delta t \tag{29}$$

Where:

$$\omega_t = \begin{bmatrix}\omega_{x_t} & \omega_{y_t} & \omega_{z_t}\end{bmatrix}$$

$$e_\omega = \begin{bmatrix}e_x & e_y & e_z\end{bmatrix}$$

Equation 29 can be expressed as equation 30, where $e_{q,\omega}$ is a zero mean white noise (process model noise). Thus, the final Kalman filter process model and process noise co-variance matrix are given by equation 31, where $\omega_{cor,t}$ is the gyroscope reading compensated for bias drift, and $E[xx^T]$ is the expectation operator.

$$q_{\omega,t} = q_{t-1} + \frac{1}{2} q_{t-1} \otimes \begin{bmatrix}0 & \omega_t\end{bmatrix}\Delta t + e_{q,\omega} \tag{30}$$

Where:

$$e_{q,\omega} = \frac{1}{2} q_{t-1} \otimes \begin{bmatrix}0 & e_\omega\end{bmatrix}\Delta t$$

$$q_{\omega,t} = q_{t-1} + \frac{1}{2} q_{t-1} \otimes \begin{bmatrix}0 & \omega_{cor,t}\end{bmatrix}\Delta t \tag{31}$$

$$Q_t = E[e_{q,\omega} e_{q,\omega}^T] = \frac{\Delta t^2}{4} q_{t-1} \otimes \begin{bmatrix}0 & \sigma^2_{\omega_x} & \sigma^2_{\omega_y} & \sigma^2_{\omega_z}\end{bmatrix} I_{4\times4} \otimes q_{t-1}^T$$

2) Sensor model: The sensor model consists of the attitude estimate obtained via the gradient descent algorithm, as well as the measurement model noise, and is given by equation 32. The measurement noise co-variance matrix is given by equation 33, where μ_t is the step size of the gradient descent algorithm. J_g is given by equation 22, ∇f_g is given by equation 23, and Σ_{acc} is the known noise characteristics of the accelerometer, given by equation 34. It is assumed that there is no correlation between the noise of the different axes of the accelerometer.

$$q_{\nabla,t} = I_{4\times4} q_{\nabla,t} \tag{32}$$

$$R_t = \frac{\mu_t^2}{||\nabla f_g||^2} J_g^T \Sigma^2_{acc} J_g \tag{33}$$

$$\Sigma_{acc} = \begin{bmatrix}\sigma_{acc_x} & \sigma_{acc_y} & \sigma_{acc_z}\end{bmatrix} I_{3\times3} \tag{34}$$

Although the centrifugal model is meant to remove some of the external acceleration from the accelerometer readings, the quadcopter can still be affected by some linear acceleration. The effects of such unanticipated acceleration are reduced by adapting the measurement noise co-variance matrix (R_t). The difference between the norm of the corrected accelerometer ($\vec{a}_{cor}$) reading and the norm of the normalised gravity vector (unity) is obtained and then used to alter the measurement noise co-variance matrix, as shown in equation 35, where ξ is given by equation 36 and R_t is the sensor noise co-variance matrix.

$$\begin{Bmatrix} R_t = \infty \ if \ |\xi| > \lambda_a \\ R_t = R_y \ if \ |\xi| < \lambda_a \end{Bmatrix} \tag{35}$$

$$\xi = ||\vec{a}_{cor}|| - 1 \tag{36}$$

The value of λ_a depends on the value of the known standard deviation of the accelerometer. Given the standard deviation of Gaussian distribution, it is possible to tell how far the measurements can spread out from the mean. Thus, if no external acceleration (external noise) is present, then the spread of the accelerometer readings is given by equation 37, where $\vec{a}_{spread_I}$ is the spread of the accelerometer readings in the earth frame and α is tuning gain. Equation 37 is only valid under the assumption that the noise in the accelerometer readings along each principle axis are uncorrelated.

$$\vec{a}_{spread_I} = \frac{\vec{g}}{||\vec{g}||} \pm \alpha \begin{bmatrix}1 & 1 & 1\end{bmatrix} \Sigma_a \ , \ \alpha = 1, 2, ...n \tag{37}$$

Thus, if the spread of the accelerometer readings in the non-accelerated scenario is known, the maximum deviation of the modulus of the accelerometer readings can be obtained using equation 38, where λ_a is the modulus of the spread of the accelerometer readings.

$$\lambda_a = ||\frac{\vec{g}}{||\vec{g}||} + \alpha \begin{bmatrix}1 & 1 & 1\end{bmatrix} \Sigma_a|| \ , \ \alpha = 1, 2, ...n \tag{38}$$

Downloaded by TU DELFT on January 5, 2022 | http://arc.aiaa.org | DOI: 10.2514/6.2022-0857

D. Gyroscope bias drift correction

Due to temperature changes and the motion of the quadcopter, the gyroscope's bias changes over time. One way to correct for the drift in bias is to estimate the bias using a Kalman filter ([3], [4], [5], [6]), but doing so leads to an increase in the number of states of the Kalman filter, which directly affects the computational cost of the overall filter. However, another filter developed by [12] utilises the integrated feedback of error. A similar approach is used in this paper for the gyroscope bias drift correction. The compensated gyroscope readings are given by equation 39, where $\omega_{gyro,t}$ is the current gyroscope reading.

$$\omega_{cor,t} = \omega_{gyro,t} - b_{\omega,t} \tag{39}$$

$$b_{\omega,t} = \rho \sum_t \omega_{e,t} \Delta t \tag{40}$$

where:

$$\omega_{e,t} = \vec{a}_{cor} \times \left(q_{t-1}^{*} \otimes \frac{\begin{bmatrix} 0 & \vec{g} \end{bmatrix}}{||\vec{g}||} \otimes q_{t-1} \right)$$

ρ is the integral gain and $\omega_{e,t}$ is the error between the corrected accelerometer readings and the projection of the gravity vector. The integral gain ρ depends on the estimated rate of change of the gyroscope bias drift. The integral constant value can be obtained in a manner similar to [11]. Equation 41 provides the value of the integral constant ρ, where $\hat{q}$ is any unit quaternion and ω_d is the estimated rate of change of the gyroscopic bias drift. If the estimated rate of change of the gyroscope bias drift is assumed to be the same along each axis of the gyroscope, equation 41 can be simplified as equation 42, where ω_d is the same along each axis of the gyroscope.

$$\rho = ||\frac{1}{2}\hat{q} \otimes \begin{bmatrix} 0 & \omega_{d_x} & \omega_{d_y} & \omega_{d_z} \end{bmatrix}|| \tag{41}$$

$$\rho = \sqrt{\frac{3}{4}}\omega_d \tag{42}$$

AEKF Algorithm

Before proceeding to the yaw estimate, the additive EKF algorithm used in the filter is provided below for the reader's convenience. The Kalman filter is initiated with the initial estimate (q_0) being the true initial attitude and the state estimation error co-variance matrix ($P_{0,0}$) as a large value matrix ($P_{0,0} = \infty$). The matrices Φ, Λ and H are identity matrices of four dimensions.

Obtain the one-step-ahead prediction using the process model (eq -26)

$$q_{\omega,t} = \frac{q_{\omega,t}}{||q_{\omega,t}||}$$

Obtain the co-variance matrix of the state prediction error

$$P_{t,t-1} = \Phi P_{t-1,t-1} \Phi^T + \Lambda Q_t \Lambda$$

Calculate the Kalman gain; R_t is obtained using equation 33

$$K_t = P_{t,t-1} H^T (H P_{t,t-1} H^T + R_t)^{-1}$$

Update measurements

$$q_t = q_{\omega,t} + K_t (q_{\nabla,t} - H q_{\omega,t})$$

Normalise q_t

$$q_t = \frac{q_t}{||q_t||}$$

Obtain the co-variance matrix of the state estimation error

$$P_{t,t} = (I - K_t H) P_{t,t-1}$$

E. Yaw estimate

To obtain the yaw estimate, the yaw rate measured by the gyroscope is integrated and added to the yaw estimate obtained via the magnetometer reading through a linear gain. The linear gain is decided using fuzzy logic to cater for magnetic disturbance. The yaw estimate obtained from the gyroscope reading via Newton integration is shown in equation 43.

$$\psi_{\omega,t} = \psi_{t-1} + \dot{\psi}_t \Delta t \tag{43}$$

Another set of yaw estimates is obtained from the magnetometer. Eclipse hypothesis compensation ([16]) is used to compensate for the roll and pitch of the quadcopter as given by equation 44.

$$\begin{bmatrix} m_{com_x} \\ m_{com_y} \\ m_{com_z} \end{bmatrix}^T = \begin{bmatrix} m_x cos(\phi_t) - m_z sin(\phi_t) \\ m_x sin(\phi_t) sin(\theta_t) + m_y cos(\theta_t) + m_z cos(\psi_t) sin(\theta_t) \\ m_x sin(\phi_t) cos(\theta_t) - m_y sin(\theta_t) + m_z cos(\phi_t) cos(\theta_t) \end{bmatrix}^T \tag{44}$$

The compensated magnetometer reading is used to calculate the yaw angle using equation 45.

$$\psi_{m,t} = acrtan(\frac{m_{com_y}}{m_{com_y}}) + \nu \tag{45}$$

where ν is the angle between the geographical north and magnetic north for the given geographical location. The final yaw estimate, which is a weighted sum of the yaw estimate obtained via the magnetometer and the yaw estimate obtained via the rate gyroscope, is obtained using a fuzzy complementary filter, as shown in equation 46.

$$\psi_t = (1 - \kappa)\psi_{\omega,t} + \kappa \psi_{m,t} \tag{46}$$

κ is the filter gain that is obtained using fuzzy logic. A fuzzy gain interpolation scheme is used, such that the gain is altered based on two criteria: Firstly, the error between the norm of the magnetic field in the inertial frame and the norm of the magnetometer readings, and secondly, the modulus of difference between the gyroscope yaw saturation point and the current gyroscope readings. The fuzzification function is given by equations 47 and 48, where fuzzifying variables are $\rho_{|m|}$ (the modulus error between the norm of the local earth's magnetic field and the norm of the measured magnetometer reading) and $|\omega_\psi|$ (modulus of the yaw rate measured by the gyroscope) respectively.

$$y(\rho_{|m|}) = \frac{e^{\frac{ln(\vartheta_m)}{\lambda_m}\rho_{|m|}} - 1}{\vartheta_m - 1} \tag{47}$$

$$y'(\rho_{|m|}) = 1 - y(\rho_{|m|})$$

$$y(\omega_\psi) = \frac{e^{\frac{ln(\vartheta_\omega)}{\omega_{\psi,sat}}|\omega_\psi|} - 1}{\vartheta_\omega - 1} \tag{48}$$

$$y'(\omega_\psi) = 1 - y(\omega_\psi)$$

The curvature of the membership function depends on the value of ϑ, which is a tuning gain. $\omega_{\psi,sat}$ is the gyro yaw rate saturation, ω_ψ is the current measured yaw rate, and λ_m is the maximum acceptable error between the norm of the local magnetic field and the norm of the magnetic field measured by the magnetometer. The value of λ_m depends on the standard deviation of the magnetometer and is given by equation 49.

$$\lambda_m = \alpha || \begin{bmatrix} 1 & 1 & 1 \end{bmatrix} \Sigma_m || \ , \ \alpha = 1, 2, ...n \tag{49}$$

The value of the maximum acceptable error (λ_m) is obtained based on a similar reasoning as the reasoning used to obtain λ_a, as given in equation 38. The error between the norm of the local earth's magnetic field and the norm of the measured magnetometer reading ($\rho_{|m|}$) is given by equation 50.

$$\begin{Bmatrix} \rho_{|m|} = ||m_t - b_e|| \ if \ \rho_{|m|} < \lambda_m \\ \rho_{|m|} = \lambda_m \ if \ \rho_{|m|} \geq \lambda_m \end{Bmatrix} \tag{50}$$

The minimum weight method, also called fuzzy intersection, is used for inference ([17]). For implementing the inference step, ideal gain values (κ_i) for the four extreme case sets need to be tuned. Due to its low computational costs, the center of gravity method ([18], [19]) is used for defuzzification, which provides the final gain for the linear complementary filter as shown in equation 51.

$$\kappa = \frac{\sum y_i \kappa_i}{\sum y_i} \tag{51}$$

An adaptive window moving average scheme is adopted to cater for yaw estimation noise. The moving average is given by equation 52.

$$\psi = \frac{\sum_i \psi_i}{i}, i = 1, 2, 3...n \tag{52}$$

An exponential function is used to calculate the window size i as shown in equation 53. The window size is directly proportional to yaw rate ($\dot{\psi}$). Furthermore, ι is a scaling constant that depends on the sensor frequency and noise.

$$i = \iota e^{-|\dot{\psi}|} \tag{53}$$

IV. Experiments, results, and discussion

The flight tests were divided into two cases: flight with and without a damaged rotor. The estimates obtained by the AFCKF are compared to three widely used mainstream filters: the filter developed by [11] (for the sake of convenience called 'Madgwick Filter'), the filter developed by [20] ('Complementary Filter'), and the filter developed by [21] ('Kalman Filter').

A. Experimental set-up

The filter was tested using data obtained from the flight of a Parrot Bepop 2 drone, which is equipped with MARG sensors. The sensor measurements were calibrated and later post-processed. The logged data were then processed through the AFCKF and the other three filters to obtain the attitude estimates of the quadcopter. The attitude estimates are compared against another set of attitude estimates which is obtained from an OptiTrack motion capture system that consists of twelve high resolution and high frame rate cameras. Using the OptiTrack system, it is possible to obtain the real-time attitude estimates of the quadcopter to an accuracy of 0.1mm.

B. Results and discussion

The attitude estimator performance is quantified by calculating the RMS of the error between the attitude estimates obtained via the OptiTrack system and the attitude estimates obtained using the attitude estimator. Furthermore, Euler representation is used to represent the roll (ϕ), pitch (θ) and yaw (ψ) of the quadcopter. Since all the filters are based on quaternion representation, the Euler angles are computed using quaternion attitude estimates and equation 9.

1) Flight with damaged rotor: In the first flight test, a quadcopter flight was conducted with one rotor fully damaged, which resulted in the quadcopter rotating about the yaw axis with a high rotational rate of about 15.5 rad/sec. The MARG sensor data obtained from the flight test were fed to the respective estimators to obtain the quadcopter's attitude estimates. Figures 2, 3, and 4 show the yaw, pitch, and roll estimation error of the different filters respectively.

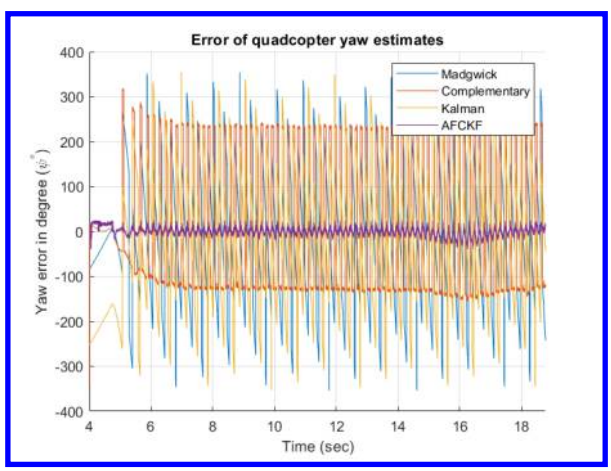

Fig. 2. Yaw estimate error of different filters [Case: damaged rotor]

Downloaded by TU DELFT on January 5, 2022 | http://arc.aiaa.org | DOI: 10.2514/6.2022-0857

Downloaded by TU DELFT on January 5, 2022 | http://arc.aiaa.org | DOI: 10.2514/6.2022-0857

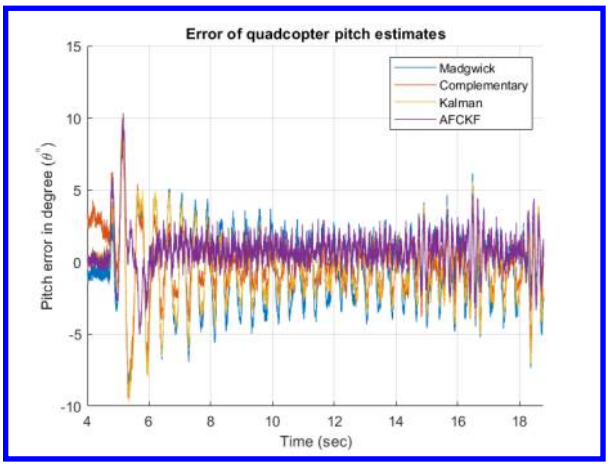

Fig. 3. Pitch estimate error of different filters [Case: damaged rotor]

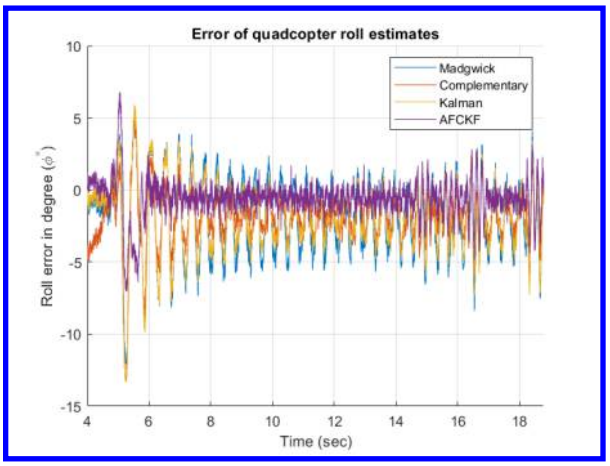

Fig. 4. Roll estimate error of different filters [Case: damaged rotor]

The RMS error, variance and execution time of the different attitude estimators are compared in tables I, II, and V respectively.

	Madgwick	Complementary	Kalman	AFCKF
Yaw (ψ°)	143.5094	164.8690	150.4092	9.8865
Pitch (θ°)	2.7121	2.0417	2.4125	1.5717
Roll (ϕ°)	3.2761	2.7165	3.0184	1.4599

TABLE I

RMS ERROR OF DIFFERENT ATTITUDE ESTIMATORS [CASE: DAMAGED ROTOR]

2) Flight without damaged rotor: A second flight test was conducted with the quadcopter's rotors being fully functional. Figures 5, 6 and 7 show the yaw, pitch and roll estimation error of different filters respectively. The RMS error, variance and execution time of the different attitude estimators are compared in tables III, IV, and V.

It can be seen from the results that in the cases of damaged rotor and the quadcopter spinning rigorously about the yaw axis, the AFCKF estimates the roll and pitch of the quadcopter more accurate than the other estimators, with an RMS error of less than 1.7 degrees and a variance of less

	Madgwick	Complementary	Kalman	AFCKF
Yaw (ψ°)	20591.4895	27182.5512	22415.3247	97.7493
Pitch (θ°)	6.9058	4.0811	5.5746	1.8775
Roll (ϕ°)	6.9263	3.4681	5.5789	1.7705

TABLE II

VARIANCE OF DIFFERENT ATTITUDE ESTIMATORS [CASE: DAMAGED ROTOR]

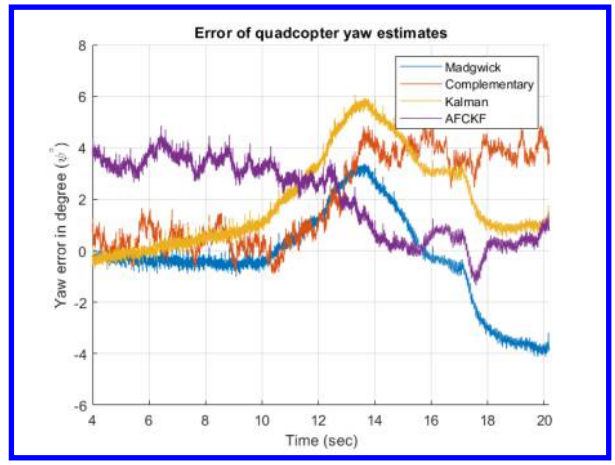

Fig. 5. Yaw estimate error of different filters [Case: without damaged rotor]

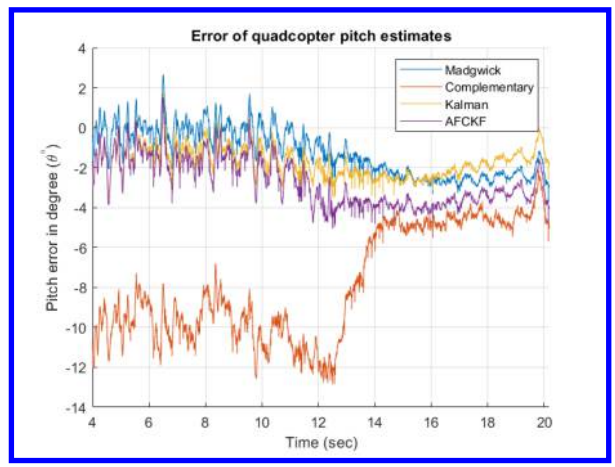

Fig. 6. Pitch estimate error of different filters [Case: without damaged rotor]

	Madgwick	Complementary	Kalman	AFCKF
Yaw (ψ°)	1.8073	2.6526	2.6571	2.4921
Pitch (θ°)	1.6893	8.2690	1.8590	2.0445
Roll (ϕ°)	1.3670	3.0333	2.9042	2.0558

TABLE III

RMS ERROR OF DIFFERENT ATTITUDE ESTIMATORS [CASE: WITHOUT DAMAGED ROTOR]

	Madgwick	Complementary	Kalman	AFCKF
Yaw (ψ°)	3.1942	3.0433	3.3033	2.2183
Pitch (θ°)	1.4312	7.8106	0.5657	1.3689
Roll (ϕ°)	0.5101	0.8680	0.1548	1.1665

TABLE IV

VARIANCE OF DIFFERENT ATTITUDE ESTIMATORS [CASE: WITHOUT DAMAGED ROTOR]

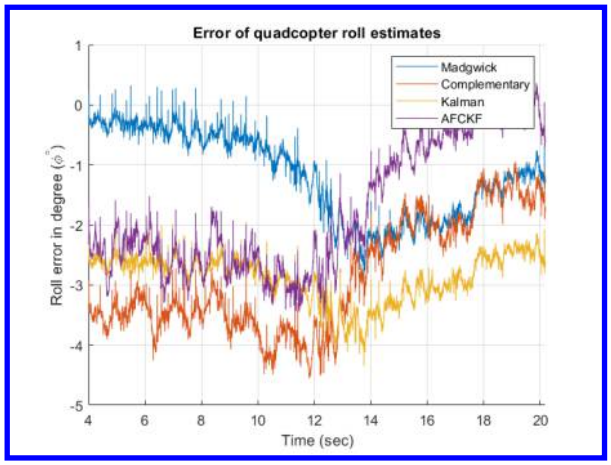

Fig. 7. Roll estimate error of different filters [Case: without damaged rotor]

	Madgwick	Complementary	Kalman	AFCKF
Time (sec)	$0.7080e^{-4}$	$5.973e^{-4}$	$4.862e^{-4}$	$1.110e^{-4}$

TABLE V

EXECUTION TIME OF DIFFERENT ATTITUDE ESTIMATORS [CASE: DAMAGED ROTOR]

than 2 degrees. For the yaw estimate, it is the only filter that is able to track the quadcopter's yaw angle. In the cases in which the rotor is not damaged, all filters show roughly similar performances with small differences that do not point to the dominance of any individual filter. Looking at the execution time, it can be observed that the Madgwick Filter is the fastest in all cases, while the AFCKF is on average 1.4 times slower than the Madgwick filter. However, it is still on average five times faster than the EKF-based filter and about six times faster than the complex complementary filter.

V. CONCLUSIONS

In this paper, a novel attitude estimator that is able to estimate the attitude of a quadcopter with one fully damaged rotor has been developed, validated, and compared to a set of mainstream estimators to evaluate its performance. The AFCKF is designed in such a way that the yaw estimates are obtained via a separate channel than the roll and pitch estimates. This prevents the yaw estimation errors from affecting the roll and pitch estimates, which is important because these estimates are essential for the quadcopter's stability. The attitude estimates obtained via the AFCKF were validated against the real-time attitude estimates obtained from the OptiTrack motion capture system. Additionally, the AFCKF was also compared against three widely used attitude estimation algorithms in order to examine its relative performance. The results show that the AFCKF is able to provide significantly better attitude estimates for flights with a damaged rotor than mainstream filters, estimating the roll and pitch of the quadcopter with an RMS error of less than 1.7 degrees and a variance of less than 2 degrees. It is the only filter that is able to track the quadcopter's yaw angle for the case of a damaged rotor, while showing only a comparatively small rise in the computational cost. In the cases in which the rotor is not damaged, the AFCKF performs as good as the other mainstream filters.

REFERENCES

[1] M. W. Mueller and R. D'Andrea, "Stability and control of a quadrocopter despite the complete loss of one, two, or three propellers," *Proceedings - IEEE International Conference on Robotics and Automation*, pp. 45–52, 2014.

[2] S. Sun, L. Sijbers, X. Wang, and C. De Visser, "High-Speed Flight of Quadrotor Despite Loss of Single Rotor," *IEEE Robotics and Automation Letters*, vol. 3, no. 4, pp. 3201–3207, 2018.

[3] J. Stephan, L. Schmitt, and W. Fichter, "Linear parameter-varying control for quadrotors in case of complete actuator loss," *Journal of Guidance, Control, and Dynamics*, vol. 41, pp. 1–15, 06 2018.

[4] D. Jurman, M. Jankovec, R. Kamnik, and M. Topič, "Calibration and data fusion solution for the miniature attitude and heading reference system," *Sensors and Actuators A: Physical*, vol. 138, no. 2, pp. 411–420, 2007.

[5] D. Gebre-Egziabher, R. Hayward, and J. Powell, "Design of multi-sensor attitude determination systems," *IEEE Transactions on Aerospace and Electronic Systems*, vol. 40, no. 2, pp. 627–649, 2004.

[6] A. M. Sabatini, "Quaternion-based extended Kalman filter for determining orientation by inertial and magnetic sensing," *IEEE Transactions on Biomedical Engineering*, vol. 53, no. 7, pp. 1346–1356, 2006.

[7] G. Wahba, "Problem 65-1: A least squares estimate of satellite attitude," *SIAM Review*, vol. 7, no. 3, p. 409, 1966.

[8] F. Markley, "Attitude determination and parameter estimation using vector observations," *Journal of the Astronautical Sciences*, vol. 36, no. 6, p. 245–258, 1988.

[9] M. D. Shuster and S. D. Oh, "Three-axis attitude determination from vector observation," *Journal of Guidance, Control, and Dynamics*, vol. 4, no. 1, pp. 70–77, 1981.

[10] J. A. Christian and E. G. Lightsey, "Sequential optimal attitude recursion filter," *Journal of Guidance, Control, and Dynamics*, vol. 33, no. 6, p. 1787–1800, 2010.

[11] S. O. Madgwick, A. J. Harrison, and R. Vaidyanathan, "Estimation of IMU and MARG orientation using a gradient descent algorithm," *IEEE International Conference on Rehabilitation Robotics*, pp. 1–7, 2011.

[12] R. Mahony, T. Hamel, and J. M. Pflimlin, "Nonlinear complementary filters on the special orthogonal group," *IEEE Transactions on Automatic Control*, vol. 53, no. 5, pp. 1203–1218, 2008.

[13] A. J. Baerveldt and R. Klang, "Low-cost and low-weight attitude estimation system for an autonomous helicopter," *IEEE International Conference on Intelligent Engineering Systems, Proceedings, INES*, pp. 391–395, 1997.

[14] J. B. Kuipers, *Quaternions and rotation sequences: A Primer with Applications to Orbits, Aerospace and Virtual Reality*. Princeton University Press, 1999.

[15] J. M. Cooke, M. J. Zyda, D. R. Pratt, and R. B. McGhee, "Npsnet: Flight simulation dynamic modeling using quaternions," *Presence: Teleoperators and Virtual Environments*, vol. 1, no. 4, pp. 404–420, 1992.

[16] Q. Tao et al., "Error compensation method for electronic compass based on best ellipse-matching error compensation algorithm," *Chinese Journal of Sensors and Actuators*, vol. 11, pp. 1499–1503, 2013.

[17] I. Beg and S. Ashraf, "Similarity measures for fuzzy sets," *Applied and computational mathematics*, vol. 8, no. 2, pp. 192–202, 2009.

[18] D. P. Madau and L. Feldkamp, "Influence value defuzzification method," *Fuzzy Systems*, vol. 3, p. 1819–1824, 1996.

[19] W. V. Leekwijck and E. E. Kerre, "Defuzzification: criteria and classification," *Fuzzy Sets and Systems*, vol. 108, no. 2, pp. 159–178, 1999.

[20] R. Valenti, I. Dryanovski, and J. Xiao, "Keeping a good attitude: A quaternion-based orientation filter for imus and margs," *Sensors*, vol. 15, no. 8, pp. 19 302–19 330, 2015.

[21] D. Roetenberg, H. Luinge, C. Baten, and P. Veltink, "Compensation of magnetic disturbances improves inertial and magnetic sensing of human body segment orientation," *IEEE Transactions on Neural Systems and Rehabilitation Engineering*, vol. 13, no. 3, pp. 395–405, 2005.

Downloaded by TU DELFT on January 5, 2022 | http://arc.aiaa.org | DOI: 10.2514/6.2022-0857